Desalination 452 (2019) 265–278

Contents lists available at ScienceDirect

Desalination

journal homepage: www.elsevier.com/locate/desal

Optimization and design of a low-cost, village-scale, photovoltaic-powered, electrodialysis reversal desalination system for rural India

David W. Bian, Sterling M. Watson, Natasha C. Wright, Sahil R. Shah, Tonio Buonassisi, Devarajan Ramanujan, Ian M. Peters, Amos G. Winter V*

Massachusetts Institute of Technology, Cambridge, MA, United States

ARTICLE INFO

Keywords:
Desalination
Electrodialysis
Photovoltaic
Optimization
Cost
India

ABSTRACT

This paper presents the cost optimization of a photovoltaic-powered electrodialysis reversal (PV-EDR) system for village-scale applications in rural India based on current component costs and performance. A PV-EDR alternative was explored because it requires half the specific energy (and thus half the power system cost), and reduces water wastage from 60% to less than 10%, compared to small-scale reverse osmosis (RO) systems for groundwater salinity levels commonly found in India. Through co-optimization of the PV and EDR subsystems, the optimal system was predicted to cost $23,420 (42% less than a system designed using conventional engineering practice). A key to the cost reduction was flexible water production that accommodates daily changes in solar irradiance with overproduction on sunny days and water buffer storage tanks. A sensitivity analysis revealed that the capital cost of the total system is most sensitive to membrane area; reducing membrane cost by 87% would half the system capital cost. The optimization method presented here, as well as the cost saving strategies of time-variant operation and load matching with solar irradiance availability, provide design strategies that are relevant to other PV-EDR architectures and general off-grid desalination applications.

1. Introduction

This paper presents the parametric theory and system modeling used to design a cost-optimized, constant voltage, and constant pumping power photovoltaic-powered electrodialysis reversal (PV-EDR) desalination system for rural India that can be built from off-the-shelf components. The EDR system was based on GE Water's electrodialysis stack model number AQ3-1-2-50/35 [1], which is a readily available product, and was previously studied, modeled, and tested by Wright and Winter [2]. The system was chosen to operate in batch mode at constant voltage and constant pumping power to accommodate varying levels of input salinity. The costs of off-the-shelf components were estimated by linear cost models, and performance estimates were based on data from OEMs and vendors. These data help establish a baseline for the lowest cost PV-EDR system that meets our desired performance requirements and can be built with readily available parts and materials. This study also investigates the cost sensitivity of PV-EDR systems to determine where future research and R&D efforts should be focused to enable further cost reductions.

The theoretical system developed in this study was designed for the Indian village of Chelluru, which lies 70 km northeast of Hyderabad. Chelluru has a population of approximately 2000 people, putting it in the median Indian village population range of 2000–5000 people [3]. The groundwater salinity is 1600 mg/L, which is within the typical Indian groundwater range of 1000–2000 mg/L. Assuming 3 L of daily water consumption per person per day [4], the median village water requirement in India is 6–15 m^3/day. While Chelluru's average daily water demand is 6 m^3/day, this study aimed to create a 10 m^3/day system in the interest of targeting the most common village size. Finally, a product water salinity of 300 mg/L was selected for satisfactory palatability, which is well below the Bureau of Indian Standards for Drinking Water recommendation of 500 mg/L [5].

1.1. Background

Brackish groundwater of salinity at or above the acceptable threshold set by the Bureau of Indian Standards for Drinking Water (500 mg/L) underlies approximately 60% of India's land area (Fig. 1) [6]. This fact makes providing desalinated water to the majority of the country imperative. As of 2015, 96.7% of Indian villages had been electrified, meaning they have some form of grid electricity [8]. However, the grid electricity in most villages is not reliable, nor do many

* Corresponding author.
E-mail address: awinter@mit.edu (A.G. Winter).

https://doi.org/10.1016/j.desal.2018.09.004
Received 16 December 2017; Received in revised form 11 August 2018; Accepted 4 September 2018

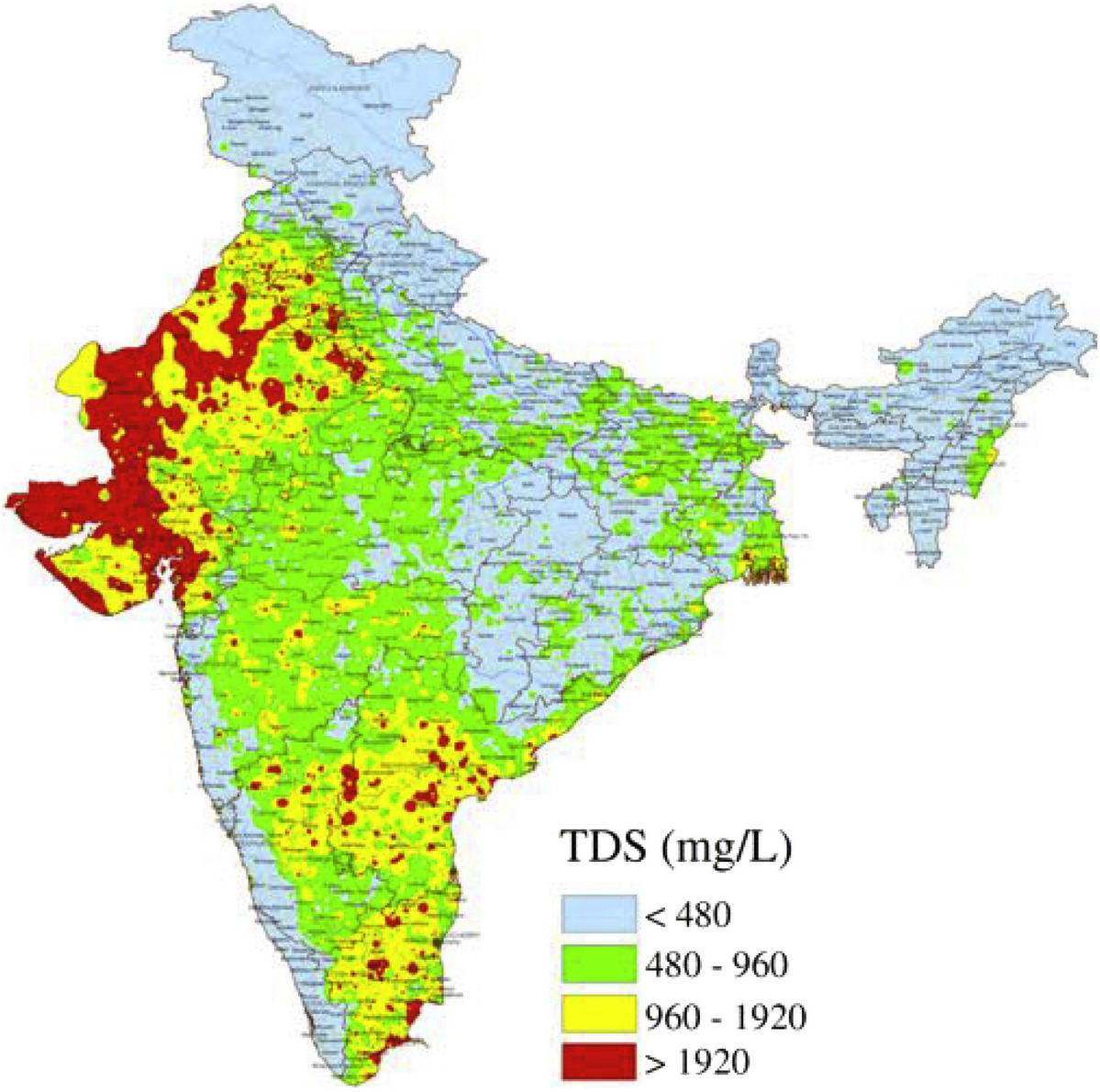

Fig. 1. Map of groundwater salinity levels throughout India [6].

households benefit from it. In 2011, only 55.3% of rural households used electricity for lighting [9], which suggests that not all the households in electrified villages have reliable access to even basic electricity. Even those that do have access to electricity experience intermittent power outages and may only have access for a few hours per day. This makes photovoltaic (PV)-powered desalination systems attractive, especially given that India has a high average daily global horizontal irradiance solar resource of 6 kWh/m^2 [10] (Fig. 2).

Tata Projects Limited, a sponsor of this research, has been working to mitigate the lack of access people have to safe drinking water sources. They have installed approximately 2200 reverse osmosis (RO) systems, all of which are grid-connected, in villages across India to desalinate the available water sources to safe drinking levels [11]. However, there is a need for more cost-effective solutions in areas where grid connection is nonexistent or unreliable. Current RO desalination solutions have been rendered cost-prohibitive for off-grid rural applications; off-grid RO systems cost more than double that of an equivalent capacity grid-connected system, at $11,250 compared to $4500. As a result, the local non-governmental organizations (NGOs) or village municipalities that purchase desalination systems are currently limited to grid-powered solutions even in semi-reliable grid electricity environments [11]. If the cost of off-grid desalination systems could be reduced, it would open up a substantial and untapped market of villages without reliable grid connection.

Electrodialysis (ED) requires less than 50% of the specific energy compared to RO to desalinate water below 2000 mg/L to a product water concentration of 350 mg/L [2]. The majority of India's brackish groundwater is below 2000 mg/L [6]. To first order, this implies that the cost of the power subsystem for PV-EDR would be half that of PV-RO. These factors suggest that ED could provide a lower-cost, off-grid brackish water desalination solution compared to RO [2]. In addition to energy savings, ED can achieve high recovery ratios of 80–90 %, compared to only 30–60 % typically achieved by the RO systems used in Indian villages [2]. The authors have observed these systems running with recoveries as low as 15%, even when blending feed and desalinated water. Adoption of ED could lead to less water waste, an important factor given that India's groundwater resources are rapidly being depleted [12-14]. Additionally, while RO membranes have an

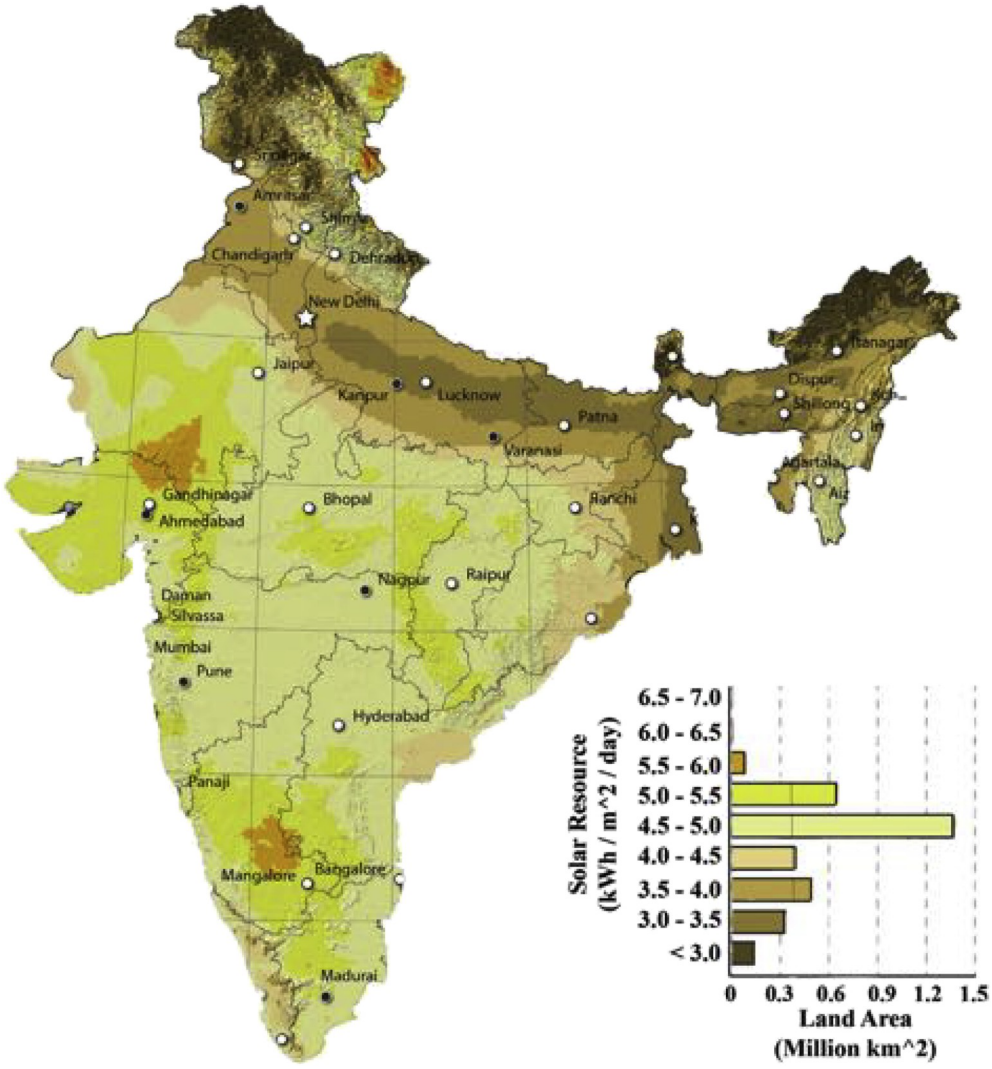

Fig. 2. Map of solar irradiation in India [7]. The high solar resource makes photovoltaic-powered systems feasible in off-grid locations in India.

expected lifetime of 3–5 years, ED membranes have an expected lifetime of 10+ years [2], which could improve maintenance and serviceability.

1.2. Prior work

The use of PV power for ED and EDR systems has been studied in the past. Laboratory-scale work has been completed to model and test a PV-ED system [15]. A number of field pilots have also been conducted. In 1987, Adiga et al. [16] completed a pilot PV-ED project in the Thar Desert, though the product water was 1000 mg/L – too brackish for our application. Additionally, PV power systems and batteries at the time were less efficient and much more expensive than they are now.

In the same year, Kuroda et al. [17] designed and constructed a batch mode PV-ED seawater desalination system in Nagasaki which operated continuously from June 1986 to March 1988 to produce 2–5 m^3 of drinking water at 400 mg/L per day. The system was meant to be optimized by matching the power consumption of the ED desalination process with the power generation from the PV panels. In 1992 Soma et al. [18] constructed a similar PV-ED system for brackish water desalination, and monitored the seasonal variation of water production.

Similar to the work presented in this paper, both systems were designed with the motivation to minimize the cost of the PV-ED desalination system. However, the tests were conducted approximately thirty years ago, produced water of a higher salinity than our targets for an Indian village, and listed no concrete cost, power, or energy consumption values for present-day comparison. Additionally, advancements in PV and battery technology have enabled different PV-ED configurations and lower costs than what was previously achievable [19]. These developments warrant a fresh, present-day investigation into cost-optimization and development of PV-EDR desalination systems.

Cost optimization of PV-powered RO desalination systems is a related area of research. Bilton et al. [20-23] investigated the impacts of location-specific environmental and demand parameters on the optimal design of modular PV-RO desalination systems using genetic algorithms. They also worked extensively on examining energy generation methods considering not only PV, but also wind turbines and diesel generators, and optimizing them together with RO systems to determine a high-reliability system configuration with the lowest lifecycle cost. Koutroulis and Kolokotsa [24] also investigated community-scale RO systems; they found for their context that a hybrid system using PV and wind power was lower cost than using a single power source.

The work presented here has similar goals in optimizing for minimal system cost while achieving high reliability of off-grid desalination systems in under-served communities. However, the performance and costs of components such as solar panels and batteries are generalized, rather than picking specific components from an inventory. Furthermore, the optimization analysis is focused on a single location for which we have water and solar irradiance data, and where a village-

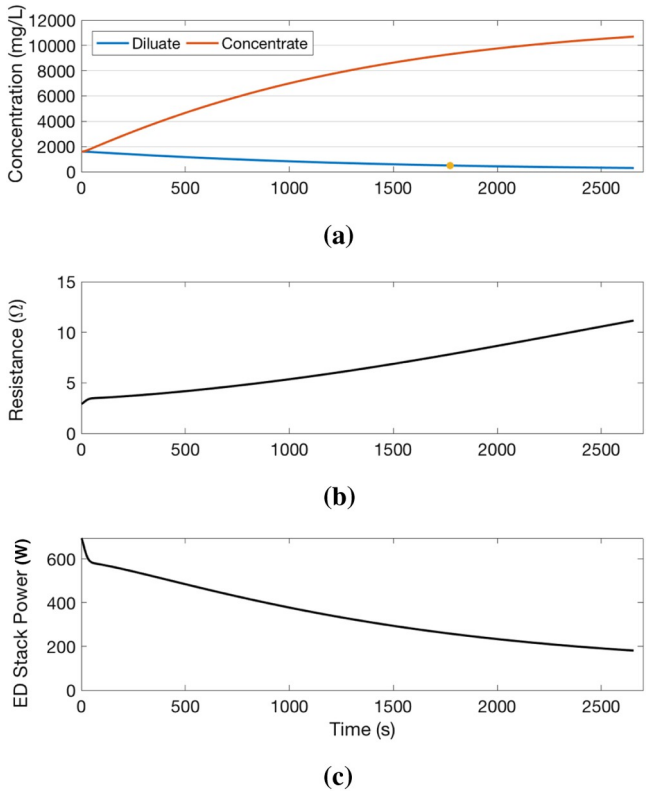

Fig. 3. The expected behavior of the cost-optimized ED system that is detailed in Section 3. (a) Concentration of the diluate (blue) and concentrate (orange) streams during the ED batch process. The yellow dot on the diluate concentration curve indicates where the diluate crosses the 500 mg/L salinity threshold that is considered acceptable by the Bureau of Indian Standards for Drinking Water [5]. (b) Cumulative electrical resistance of the ED stack during the ED batch process. (c) ED stack power draw during the ED batch process. As (a) the diluate concentration decreases, (b) the overall resistance of the stack increases, causing the current and thus (c) the stack power to decrease during the batch process. The variables and parameters assumed to create these figures are listed in Table 1.

scale RO system is currently running. The novelty of this work lies in the parametric theory to design the lowest cost, constant voltage and pumping power PV-EDR system that can be built from off-the-shelf parts. The major insights from the study are that co-optimization of the PV and ED subsystems leads to lower cost than a serial optimization of each, and that flexible operation of the system allows for reduced battery costs by overproducing water on sunny days and storing it in tanks. The knowledge presented herein is generalizable to many locations and applications beyond Chelluru, India, and will enable engineers to design cost effective PV-EDR systems for other size scales, salinities, and contexts.

2. PV-EDR system model

2.1. Electrodialysis reversal batch system behavior

In this study, EDR operated in a batch mode configuration is examined. EDR operates identically to ED, with the addition of a periodic reversal of the diluate and concentrate streams as well as the stack voltage polarity. In batch mode, the water in the diluate and brine tanks is recirculated through the ED stack continuously until the desired diluate salinity is reached. After a reversal, the diluate streams flow in the channels where the concentrate streams flowed previously, and vice versa. In practice, this is done by using valves to redirect water flow and reversing the polarity of the applied voltage. For this work, the ED stack used is manufactured by GE Water (model number AQ3-1-2-50/35).

The models for predicting the performance and behavior of batch electrodialysis systems utilized in this study have been developed and validated by Wright et al. [25]. In addition, it is suggested that the reader review Wright [26], Ortiz [27], Strathmann [28], and Tanaka [29] for a more complete understanding of the electrodialysis process. The major concepts and analytical relationships behind ED are summarized here to highlight their relevance to the overall optimization of the PV-EDR system. It is important to note that these models assume that the dissolved salts in the water are purely monovalent (from NaCl). Wright et al. [25] have experimentally demonstrated that NaCl is a good approximation for real groundwater for accurately predicting the performance of an ED system using the following models.

2.1.1. Mass transfer

The mass transfer of ions from one stream to another was modeled using Ohm's law, where the electric potential is the voltage applied across the ED stack, the current is the ion movement, and the resistance is the electrical resistance of the membranes and the streams. Eqs. (1) and (2) are the mass balance equations for the concentrate and diluate streams, respectively [27]:

$$N_k V_k \frac{dC_{conc}}{dt} = Q_{conc} C^0_{conc} - Q_{conc} C_{conc} + \frac{N_k \phi I}{zF} - \frac{N_k A D_a (C^{wa}_{conc} - C^{wa}_{dil})}{l_a} - \frac{N_k A D_c (C^{wc}_{conc} - C^{wc}_{dil})}{l_c} \quad (1)$$

$$N_k V_k \frac{dC_{dil}}{dt} = Q_{dil} C^0_{dil} - Q_{dil} C_{dil} + \frac{N_k \phi I}{zF} + \frac{N_k A D_a (C^{wa}_{conc} - C^{wa}_{dil})}{l_a} + \frac{N_k A D_c (C^{wc}_{conc} - C^{wc}_{dil})}{l_c}, \quad (2)$$

where N_k is the number of cell pairs, V_k is the volume of the streams, C^0_{conc}, C^0_{dil}, C_{conc}, and C_{dil} are the concentrations of the concentrate and diluate streams at the inlet and outlet of the electrodialysis stack, respectively, Q_{conc} and Q_{dil} are the volumetric flow rates, ϕ is the current efficiency, I is the current, z is the sign and charge of the ion, F is the Faraday constant, A is the active membrane area, D_a and D_c are the average diffusion coefficients of NaCl in the anion and cation exchange membranes, respectively, l_a and l_c are the thicknesses of the anion and cation exchange membranes, respectively, t is the time, and C^{wa}_{conc}, C^{wa}_{dil}, C^{wc}_{conc}, C^{wc}_{dil} are the concentrations on the surface of the anion and cation exchange membranes at the boundaries of the concentrate and diluate streams, respectively. The terms in Eqs. (1) and (2) represent flow of ions at the inlet and outlet of the channels, the ion flow due to the current, and the diffusion of ions across the membranes due to the concentration gradient between the concentrate and diluate streams, respectively.

Fig. 3 shows the expected behavior of an ED system that has the parameters outlined in Table 1. As the concentrations of the concentrate and diluate streams change (Fig. 3a), their electrical resistances change. Due to the nonlinear relationship between resistivity and ion concentration, the diluate channels become the dominant resistance in the circuit, increasing electrical resistance overall (Fig. 3b). During a batch process at constant voltage, this increasing resistance causes a decrease in current over time, slowing the desalination process

Table 1
ED variables and parameters assumed for Fig. 3.

ED variables and parameters	Quantity
# ED cell pairs	62
Stack voltage	45 V
Batch size	0.42 m^3
Feed water salinity	1600 mg/L

of removing ions from the diluate stream. This causes the electrical power over the course of a batch to decrease proportionally with the current (Fig. 3c).

2.1.2. Limiting current density

If the applied voltage is too high, then at some point during the batch desalination process the ion concentration at the membrane surfaces in the diluate channels approaches zero. The condition during which this occurs is called limiting current density, which can result in electrolysis of the water molecules, causing harmful production of hydrogen gas and decreased pH levels of the desalinated water. The ED system should be designed as to avoid reaching limiting current density at any point during the batch process to ensure safe drinking water quality. The limiting current density i_{lim} [A/m^2] is estimated using

$$i_{lim} = \frac{C_{dil}^{bulk} zFk}{T_{mem} - t^+}, \tag{3}$$

where C_{dil}^{bulk} is the concentration of the bulk diluate solution, t^+ is the transport number of the ion in the bulk solution, and T_{mem} is the transport number of the ion in the membrane. k is the boundary-layer mass transfer coefficient and increases with the linear flow velocity in the channels, causing a proportional increase in the limiting current density. In this analysis, the flow channels, membrane geometry and linear flow velocity are held constant, meaning that the pressure drop due to flow through the channels is also constant. Holding these factors constant means that the limiting current density varies only with C_{dil}^{bulk}, which decreases over the course of the desalination process.

2.1.3. Electrodialysis system design considerations

For the purposes of this work, the desalinated water production rate and power profiles for the entire desalination batch process are the key factors that drive system cost. Desalination rate can be varied by changing (1) the applied voltage across the EDR stack and (2) the number of cell pairs. Assuming a constant linear flow velocity through each channel, the number of cell pairs effectively changes the number of channels and thus the volumetric flow rate. The range of optimal linear velocities for the spacers in the ED stack is 6–12 cm/s [1,30]. Because pressure drop per unit length of the spacer exhibits quadratic growth with increasing linear flow velocity, we chose to design our system to run at 6 cm/s primarily because it requires less pumping power per unit flow rate, which in turn lowers system cost through decreased battery and photovoltaic panel requirements. Additionally, lower linear flow rates are correlated with greater salt removal per unit length of spacer, which is beneficial for effective desalination [30].

The applied voltage and number of cell pairs therefore also determine the power and energy profiles associated with the desalination process. Varying these values only produces small differences in the total energy required per volume of drinking water. Assuming limiting current is not reached, the power delivered to the stack is proportional to the applied voltage and stack current, and the pumping power is proportional to the number of cell pairs. The maximum number of cell pairs in this study was limited to 170, which is the number of cell pairs available in the fully assembled GE Water ED stack. This study originally encompassed ED stacks with up to two electrical stages and two hydraulic stages per electrical stage (GE Water's standard configuration); the optimization quickly narrowed the solution space to one electrical stage with one hydraulic stage. Therefore, for the purposes of simplifying the optimization study, the ED system architecture presented here has been optimized for one electrical stage with one hydraulic stage. The recovery of the system was chosen to be 80% to minimize water wastage, and is within the capabilities of electrodialysis. In practice, the ED system designed here would have UV post-treatment, administered when product water is distributed from the storage tank to a user, to decontaminate the water from biological pathogens. The cost of a UV system is relatively small compared to the other major cost elements included in this analysis, and thus was not included in the optimization.

2.2. Photovoltaic power system behavior

The power production of the PV array and the power consumption of the electrical load were used to determine the sizing of the battery bank through an energetic analysis. The energetic models used here were developed by Watson et al. [31,32].

Solar irradiance and temperature data for the region of Chelluru, India, in the year 2014 were used as a reference year's weather data throughout this work. These are semi-empirical satellite-based data from the National Solar Radiation Database (NSRDB) SUNY database [33]. The efficiency, η_{PV}, of the solar panels at each time interval was calculated using

$$\eta_{PV}(t) = \eta_{PV,nom}[1 + \alpha_p(T_{amb}(t) + k{\cdot}GHI(t) - T_{std})], \tag{4}$$

where $\eta_{PV,nom}$ is the nominal efficiency of the panels (15% was assumed in this analysis), α_p is the temperature coefficient [1/K] (−0.42% assumed in this analysis [34]), $T_{amb}(t)$ is the ambient temperature, k is the Ross coefficient, which relates irradiance to module temperature (k = 0.025 K·m^2/W was used for this analysis [35]), $GHI(t)$ is the global horizontal irradiance, and T_{std} is the standard testing temperature of 25°C. The power produced by one square meter of photovoltaic panels, $P_{PV,1m}$, was calculated by multiplying the instantaneous PV efficiency, η_{PV}, by the instantaneous global horizontal irradiance $GHI(t)$. The PV array power output, P_{PV}, is simply the product of $P_{PV,1m}$ and the area of the PV array. As a first-order constraint, the output of the PV panels must be enough to produce the total amount of energy required to desalinate water over the yearly cycle. By increasing the PV area beyond this theoretical minimum, the energy storage requirements can be significantly reduced.

The energy stored in the battery bank during charging was calculated using

$$E_{stored}(t) = E_{stored}(t-1) + \Delta t{\cdot}\left[P_{PV}(t) - \frac{P_{load}(t)}{\eta_{conv}}\right]{\cdot}\eta_{batt}, \tag{5}$$

and the energy stored during discharging was calculated using

$$E_{stored}(t) = E_{stored}(t-1) + \Delta t{\cdot}\left[\frac{P_{load}(t)}{\eta_{conv}} - P_{PV}(t)\right], \tag{6}$$

where E_{stored} is the energy stored in the batteries, Δt is the time interval in seconds (300 s was used in this analysis), P_{load} is the power being consumed by the electrodialysis process and the pumps, η_{conv} is the efficiency of the power converter, and η_{batt} is the battery charge/discharge efficiency. Temperature effects were not considered in the battery operation, which is acceptable because the battery bank of the PV-EDR system was assumed to be stored out of direct sunlight.

The desalination process uses energy to produce potable water; storing it can serve as a secondary energy storage medium in addition to energy storage in batteries. Under certain conditions, utilizing product water storage in addition to energy storage can allow for system cost reductions. This technique was utilized in the optimization of the PV-EDR system.

2.3. PV-EDR coupled behavior and simulation model

A PV-EDR model was developed using the theory from the previous subsections to inform the design of cost-optimized PV-EDR systems for a specific location, and to specifically optimize the off-grid, village-scale PV-EDR system for a median-sized village in India. This model is composed of four modules: the electrodialysis module, the pump selection module, the power system and storage module, and the cost module. It was designed to take location-specific parameters and specified values of design variables as inputs, and produce a system capital

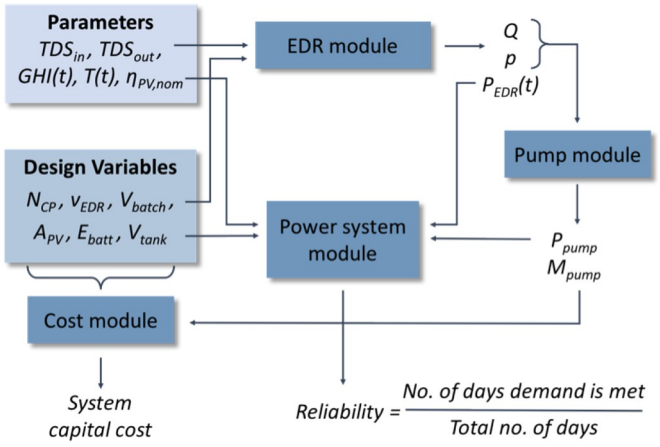

Fig. 4. Flowchart of the PV-EDR simulation, where TDS_{in} is the input salinity, TDS_{out} is the output salinity, *GHI* is the global horizontal irradiance, *T* is temperature, (*t*) denotes a function of time, $\eta_{PV,nom}$ is the nominal PV efficiency, N_{CP} is the number of cell pairs, v_{EDR} is the stack voltage, V_{batch} is the batch volume, A_{PV} is the area of the PV array, E_{batt} is the battery capacity, V_{tank} is the water storage tank volume, *Q* is the flow rate, *p* is the pressure, P_{EDR} is the power required for EDR over a batch, P_{pump} is the pumping power, and M_{pump} is the pump model.

cost and output reliability for the specific design. This process flow is depicted in Fig. 4.

2.3.1. Electrodialysis module

The EDR module simulates the water desalination process. To do so, it takes the feed water salinity TDS_{in}, desired output water salinity TDS_{out}, and desired average daily water production as fixed inputs. The number of cell pairs N_{CP}, applied stack voltage v_{EDR}, and batch size V_{batch} are taken as design variables. The module then calculates and outputs the duration of a batch, water production rate, power profile P_{EDR}, whether limiting current density was exceeded, and the flow rate and pressure required of the pumps. A design fails in the EDR module if the limiting current density is exceeded or if the desired salinity of the batch is not reached in sufficient time to allow the daily water production to be achievable.

2.3.2. Pump selection module

Based on the flow and pressure requirements of the ED system, an optimal pump must be chosen that minimizes cost, power consumption, and difference between the actual and the desired flow and pressure. A database was created from which to select specific pump models due to a poor correlation between pump performance metrics and cost (Appendix A).

The pump selection module takes the system curve as well as the desired pressure and flow rate of the EDR system as inputs. These are compared to the pump curves of the pumps in the database. The intersection points represent the expected actual operating point of the pump. A pump selection metric (PSM),

$$PSM = C_{pump} + 3P_{pump} + 750|Q_{desired} - Q_{actual}|, \quad (7)$$

was created to evaluate the quality of choice of the pump based on pump cost C_{pump}, power consumption P_{pump}, and the difference between the flow rate at the intersection Q_{actual} to the desired flow rate $Q_{desired}$. The pump in the database with the lowest *PSM* value for the desired flow rate and pressure is chosen for the design. Minimizing the cost of the pump directly translates to capital cost reductions of the PV-EDR system. Minimizing power consumption reduces the energetic demands of the system, leading to decreased amounts of required batteries and photovoltaic panels, which in turn leads to lower system capital cost. Minimizing the difference between the actual and desired flow rate will decrease the likelihood of affecting the desalination process due to a greatly different flow rate.

The cost coefficient in Eq. (7) is 1 because it has a direct correlation to the overall system capital cost. The power coefficient is 3 because it is estimated that a small microgrid costs $3/W of power generating capacity [36,37], and it is estimated here that the power consumption of the pump would add approximately $3/W of cost to the PV power system, and thus to the total PV-EDR system capital cost. The flow rate difference coefficient of 750 was determined iteratively, such that the flow differential would be unlikely to exceed 0.1 m^3/hour and thus would be unlikely to significantly change the predicted pumping pressure required or the desalination process.

2.3.3. Power system and storage module

Solar is an intermittent power source that varies on daily and seasonal scales. A PV-powered system must have the energy storage capacity to provide the required power to the load despite fluctuations on the daily scale (such as clouds and nighttime operation) and variations on the yearly scale, such as lower solar irradiance during the winter season. A combination of PV panels and batteries can meet the power profile of a prolonged electrical load. The optimal sizing of the PV array and battery pack depends on location-specific weather data such as irradiance and ambient temperature, the power profile of the load, and the relative cost of PV and batteries.

The power system module uses irradiance *GHI*(*t*) and temperature *T*(*t*) data time resolved into five-minute intervals over a year, and nominal PV efficiency $\eta_{PV,nom}$, as parameter inputs to Eq. (4) to calculate the estimated PV efficiency $\eta_{PV}(t)$. Design-specific values of PV array area A_{PV}, battery capacity E_{batt}, and water storage tank volume V_{tank}, as well as the power profiles of the EDR unit $P_{EDR}(t)$ and pump $P_{pump}(t)$ are input into the module. The energy flow into and out of the batteries and the water flow into and out of the water storage tanks are simulated over the reference year period, and an output reliability corresponding to the percentage of days over the year for which water supply meets demand was calculated. The simulation decides when to run a batch, simulate the charging and discharging of the batteries, and simulate the water withdrawal over the course of a day according a logic tree (Fig. 5). Within the simulation, the battery maximum discharge depth allowed is 50%, a value selected to prolong battery lifetime.

2.3.4. Cost module

The cost module calculates the cost of the PV-EDR system based on the system design variables and the selected pump according to Eq. (8) using the costs in Table 2.

$$C_{sys} = C_{PV}A_{PV} + C_{batt}E_{batt} + C_{tank}V_{tank} + C_{CP}N_{CP} + 2C_{elec} + 2C_{pump}, \quad (8)$$

where C_{sys} is the system capital cost; C_{PV}, C_{batt}, C_{tank}, C_{CP}, C_{elec}, and C_{pump}, are the cost of the PV array, battery bank, water storage tank, membrane cell pairs, electrodes, and pumps, respectively; and A_{PV} is the area of the PV array, E_{batt} is the battery capacity, V_{tank} is the water storage tank volume, and N_{CP} is the number of membrane cell pairs. The cost of PV, batteries, and water storage were all determined based on local or commonly used component costs. The cost of ED cell pairs and electrodes ($2000 per electrode) are based on estimates from supplier quotations for the GE Model Number AQ3-1-2-50/35 ED stack [38]. The membranes are approximately 0.47 m^2, so a cost of $150/cell pair translates approximately to $160/$m^2$ (two membranes per cell pair).

The cost of an AC/DC inverter varies widely between the United States and India, and to the authors' knowledge, there is no generalized or formulaic way to estimate the cost of an inverter. Due to both of these considerations, it was prudent to exclude the inverter cost in the cost module, though it would certainly add to the actual total system cost. Additionally, a chemical injection pump may be desirable in

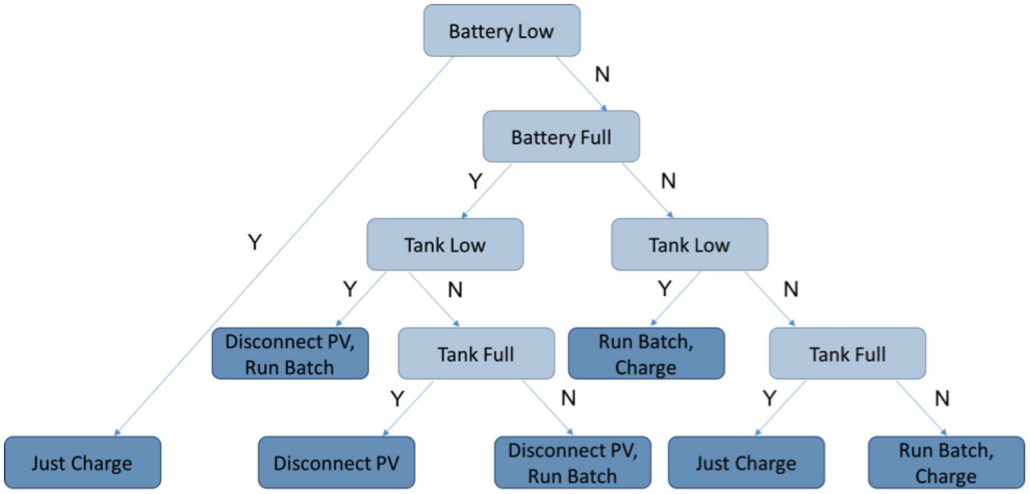

Fig. 5. Logic tree for the power system module, detailing the conditions for charging the batteries and running an EDR batch.

Table 2
Design variables that define a PV-EDR system and their associated costs per unit.

Design variable	Symbol	Cost
PV area	A_{PV}	\$98/m^2 [39]
Battery capacity	E_{batt}	\$150/kWh [39]
Water storage volume	V_{tank}	\$110/m^3 [40]
# ED cell pairs	N_{CP}	\$150/cell pair [38]
Stack voltage	v_{EDR}	From optimization
Batch size	V_{batch}	From optimization
Pump model	M_{pump}	From optimization

implementation for the purpose of adding chemicals like antiscalant, though this would not be a major cost driver and was thus excluded from the cost module.

2.3.5. System simulation model

The performance of a PV-EDR design over a reference year was simulated in MATLAB [41]. The input parameters for the simulation given in Table 3 are primarily targeted at the median-sized Indian village, though the input salinity and solar irradiance are specific to Chelluru. The solar irradiance and temperature data used for all simulations were obtained from the National Solar Radiation Database (NSRDB) SUNY database for the village of Chelluru, India in 2014 [33], and interpolated to five-minute intervals. All references to water production reliability are defined as the percentage of days that the simulation predicted the system would be able to provide the needed quantity of water under the weather conditions of the 2014 reference year. The water distribution model assumes 0.25 m^3 of water is collected by users instantaneously every 15 min over the course of 10 h during the day, resulting in 10 m^3 per day, with the simplifying assumption that there is no seasonal variability in water demand.

Table 3
Input parameters for the PV-EDR simulation, specific to conditions in Chelluru, India.

Parameter	Symbol	Value
Input salinity	TDS_{in}	1600 mg/L
Output salinity	TDS_{out}	300 mg/L
Daily water production	V_{prod}	10 m^3
Water production reliability	r_{req}	100%
Solar irradiance	$GHI(t)$	2014 GHI data
Ambient temperature	$T(t)$	2014 data
Nominal PV efficiency	$\eta_{PV,nom}$	15%

Just as the power production and availability of the PV system can be tuned by sizing the panels and batteries, the power consumption of the ED system can be tuned by selecting the quantity of membrane cell pairs, operating voltage, batch size, tank size, and pump model. By jointly adjusting power production and power consumption, the power profiles can be matched in such a way as to optimize the overall system for minimum cost. Harvested energy can be (1) stored in batteries for later use or (2) used immediately for desalination, storing the excess water in tanks to meet customer demand at times of low irradiance.

Incorporating water storage tanks as a secondary storage medium to batteries can reduce the battery energy storage requirement for the system as well as the overall cost of the system [31,32]. Because of this fact, through exploration of the design space it was observed that the optimizer tended to maximize water storage capacity, as it was cheaper to produce and store excess water on days with high solar irradiance than to store the excess energy in batteries.

3. PV-EDR system optimization

When the model described in the previous section is coupled to a particle swarm optimization (PSO) [42] algorithm, multiple designs are randomly initialized and then varied and eventually converge on a low-cost design with acceptable reliability. A PV-EDR design was characterized as a combination of the design variables listed in Table 2. Due to the coupled nature of the PV and EDR subsystems, it is nontrivial to determine what configuration of the ED stack, pump models, and quantities of PV panels, batteries, and water storage tanks will result in the lowest capital cost system, and a full-factorial study would be too time-consuming and inefficient. Coupling an optimizer algorithm with the PV-EDR performance models can more efficiently determine a near-cost-optimal combination of these components and the accompanying operational specifications. In this study, PSO was utilized because of its suitability for searching a complex design space using stochastic methods, and the simplicity of implementation. PSO is a population-based algorithm that initializes “particles” that move through a design space until the population converges on a local or global optimum.

For the purposes of optimization, days that failed to supply the water demand were penalized by adding \$1000 to the system cost for each of the N_{failed} failed days. Thus, the \$1000 per failed day penalty indicates to the optimizer how much adjustment a design needs in order to meet the desired reliability. This adjusts Eq. (8) to

$$C_{sys} = C_{PV}A_{PV} + C_{batt}E_{batt} + C_{tank}V_{tank} + C_{CP}N_{CP} + 2C_{elec} + 2C_{pump} + 1000N_{failed}. \quad (9)$$

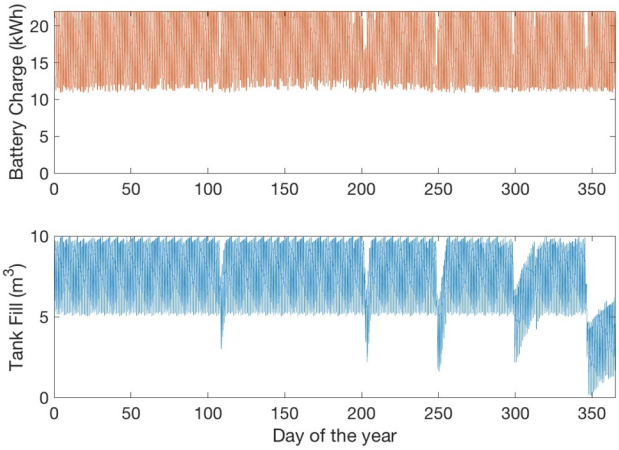

Fig. 6. Simulated battery charge level and tank fill level for the optimized PV-EDR design during the reference year.

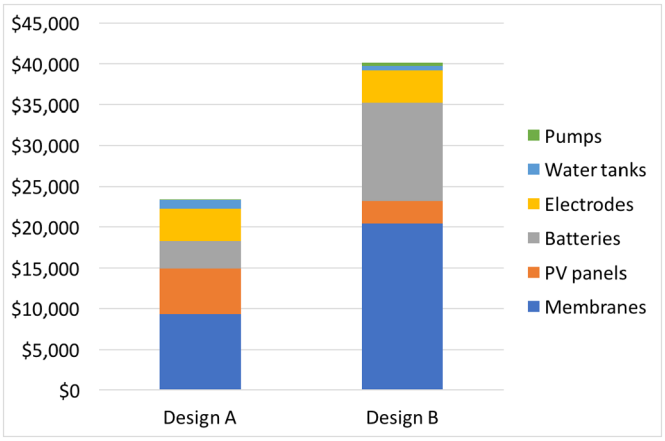

Fig. 7. Comparison of cost breakdowns for Design A, the optimized system ($23,420 total), and Design B, the conventionally designed system ($40,138). Design B has a much larger ED stack which contributes significantly to its capital cost, as well as a much larger battery bank.

3.1. The optimized PV-EDR system

PSO was used in MATLAB to determine a cost-optimal PV-EDR design for any given set of parameters and design variables. Due to the stochastic nature of PSO, the optimization converged to a different solution every time it was run. To identify the likely global minimum solution, the optimization was run several times to identify the most promising regions of the design space. The design variable bounds were constricted so the optimization was constrained to exclusively search in those narrowed regions of the design space to find the cost-minimum design.

The simulated performance of the optimized PV-EDR design over the reference year is shown in Fig. 6. During times of low irradiance when the battery was depleted to the minimum allowed level of 50% charge, the water stored in the tank would begin to be withdrawn, serving as a water demand buffer until the batteries could regain charge. This mode of operation allowed the simulated system to provide the daily water requirement of 10 m^3.

Table 4 shows the results of the PV-EDR optimization for a system satisfying the design parameters listed in Table 3, and the cost breakdown of components is shown in Fig. 7.

3.1.1. Levelized water cost

The levelized cost of water is typically calculated using the full system capital costs, facility costs, operation and maintenance costs, component replacement and other variable costs, and interest rates [43]. For the optimized system described in the previous subsections, only the initial major system components and their replacement costs are considered, as many of the other factors such as transportation, construction, installation, and operation costs are still unknown. The partial levelized water cost estimation presented here assumes a system lifetime of 20 years, time-independent component costs, and unfailing operation over the full system lifetime. The components considered, their associated costs, assumed lifetimes, and the estimated numbers of times the components are purchased (including the initial purchase) over the course of 20 years are given in Table 5.

During its 20-year lifetime, the system is assumed to produce 73,000 m^3 of water (10 m^3 a day for 365 days a year for 20 years). With a lifetime cost of $47,063, this results in a partial levelized water cost of $0.645/$m^3$, compared to $0.73/$m^3$ for the 500 LPH on-grid RO system installed in Chelluru by Tata Projects (Table 6). Though many factors that are not included would add to these costs, it is still a reasonable

Table 4
Design variable values for the lowest-cost PV-EDR system found through PSO iteration. The total system cost based on these optimized system design variables was $23,420.

Design variable	Symbol	Quantity
PV area	A_{PV}	57.5 m^2
Battery capacity	E_{batt}	22 kWh
Water storage volume	V_{tank}	10 m^3
# ED cell pairs	N_{CP}	62 cell pairs
Stack voltage	v_{EDR}	45 V
Batch size	V_{batch}	0.42 m^3
Pump model	M_{pump}	Kirloskar Wonder III (x2)
Total cost		$23,420

Table 5
The components considered, their associated costs, assumed lifetimes, and the estimated numbers of times the components are purchased (including the initial purchase) over the course of 20 years for the cost-optimized PV-EDR system. The lifetime cost is $47,063 for a lifetime water production of 73,000 m^3 of water, resulting in a partial levelized water cost of $0.645/$m^3$.

Components	Quantity	Cost	Lifetime (years)	# of Times purchased
PV panels	57.5 m^2	$98/$m^2$	20+	1
Batteries	22 kWh	$150/kWh	5	4
Water storage	10 m^3	$110/$m^3$	20+	1
ED electrodes	2	$2000/electrode	10	2
# ED cell pairs	62 cell pairs	$150/cell pair	10	2
Pump	2	$44/each	3.5	6
Total lifetime cost			$47,063	

Table 6
The components considered, their associated costs, assumed lifetimes, and the estimated numbers of times the components are purchased (including the initial purchase) over the course of 2.5 years for the Tata Projects on-grid RO system currently installed in Chelluru. The 2.5-year lifetime cost is $4,384 for a production quantity of approximately 6000 m^3 of water, resulting in a partial levelized water cost of $0.73/$m^3$.

Components	Quantity	Cost	Lifetime (years)	# of Times purchased
RO membranes	3	$267	2.5	1
Cartridge filters	3	$2.5	0.038	66
Grid electricity cost	1	$100/month	0.083	30
Pump	2	$44/each	3.5	1
Total lifetime cost			$4384	

value compared to the \$0.58/m^3 water cost claimed for another brackish water ED system [44,45], given that the conditions under which that cost was calculated are also not fully known.

4. Discussion

4.1. Comparison to PV-EDR system designed using conventional methods

For comparison, let the optimized design found in the previous section be referred to as Design A, in which the optimization and design of the PV and EDR subsystems were performed jointly, resulting in the design of a co-optimized system. On the other hand, let Design B be a PV-EDR system designed using the conventional method of designing the load – in this case, the ED desalination system – and then the power system sequentially.

Design A has been detailed in the Section 3. For Design B, the EDR system was sized based on two criteria: the daily water production requirement of the median Indian village of 10,000 L(10 m^3), and an average operation period of 8 h per day (consistent with a typical workday, and with the operation period of the on-grid RO system currently installed in Chelluru). Correspondingly, the nominal flow rate of product water was chosen to be 1250 L per hour (LPH). The electrodialysis model described in Section 2 was used to find the lowest-cost ED stack (when considered independently from the PV system) capable of producing 10 m^3 per day at a 1250 LPH production rate. This high production rate requires approximately a proportional increase of 2.5 times the number of electrodialysis cell pairs and applied stack voltage compared to Design A (140 cell pairs and a stack voltage of 100 V). However, the number of cell pairs was slightly reduced by increasing the applied voltage per cell pair, resulting in 136 cell pairs and a stack voltage of 98 V. This modification was motivated by the decreased cost of the EDR system by decreasing the number of cell pairs. The batch size was chosen to be 1 m^3 because it is a commonly used tank size and it could be desalinated and sent to the water storage tank in less than an hour. A suitable pump was suggested by Tata Projects, our industry partner, based on pumps they commonly use for their water purification systems and their knowledge of the local market. This EDR design had a daily energy requirement, $E_{EDR,d}$, of 20 kWh per day.

To design the power system, a battery capable of providing two days of backup was used based on suggested practice [46]. This resulted in an energy usage requirement of $2 \cdot 20$ kWh $= 40$ kWh, resulting in a total battery capacity of 80 kWh assuming a 50% discharge depth. India's average daily global horizontal irradiance solar resource for the region under consideration, $E_{PV,d}$, is 6 kWh/m^2 per day [10]. This average was used to calculate the required area of PV panels according to

$$A_{PV} = 1.3\frac{E_{EDR,d}}{\eta_{PV} E_{PV,d}}, \tag{10}$$

where 1.3 is a scaling factor to account for losses [46] and η_{PV} is calculated using Eq. (4). In this case, $A_{PV} = 28.9$ m^2. For water storage, an industry standard 5 m^3 tank was assumed. The design variables of Design B are shown in Table 7 and the total system cost was calculated using Eq. (8) to be \$40,138. The breakdown of cost by system components is shown in Fig. 7.

Table 7
Design variables for Design B, the PV-EDR system found through conventional design methods. The total system cost based on these design variables was \$40,138.

Design variable	Symbol	Quantity
PV area	A_{PV}	28.9 m^2
Battery capacity	E_{batt}	80 kWh
Water storage volume	V_{tank}	5 m^3
# ED cell pairs	N_{CP}	136 cell pairs
Stack voltage	v_{EDR}	98 V
Batch size	V_{batch}	1 m^3
Pump model	M_{pump}	CNP CHL 2-30 (x2)
Total cost		\$40,138

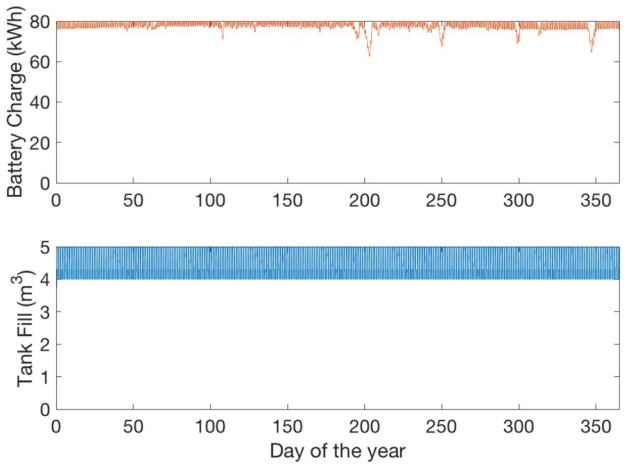

Fig. 8. Simulation of the battery charge level and tank fill level for Design B during the reference year.

A simulation of the performance of Design B over the reference year is shown in Fig. 8. It is evident that the battery capacity is highly oversized, such that the water storage is at no point utilized for buffering. The variation in the tank volume is due to the water usage and the 1 m^3 batch size.

4.2. Cost sensitivity analysis

The system models and optimization tools were also used to investigate the sensitivity of system capital cost to water output reliability and individual component cost. Each data point was produced by running the PSO optimization multiple times to find the associated total system cost. It is important to emphasize that each data point differs not only in cost, but also in system configuration.

As the output reliability constraint of 100% is relaxed, the capital cost drops quickly at first (Fig. 9), suggesting that just a few days of low sunshine are responsible for a disproportionate fraction of the system cost.

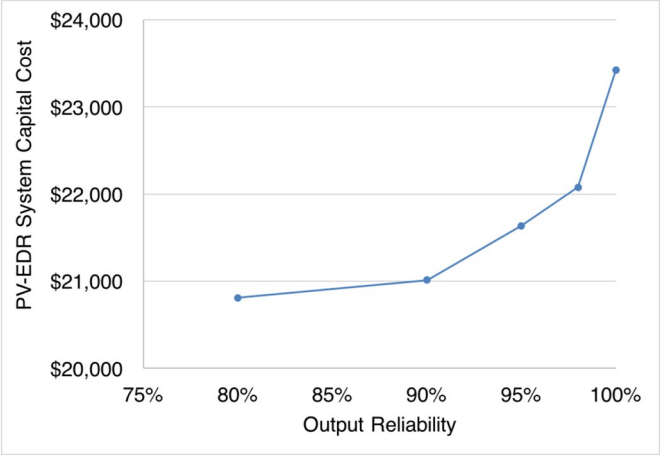

Fig. 9. Sensitivity of optimized PV-EDR system capital cost to daily water output reliability. Reducing output reliability from 100% to 98% (7 days of the year in which the system fails to provide 10 m^3) produces an optimized cost reduction of 5.7% from \$23,420 to \$22,076, a relatively sharp drop compared to the 10.3% cost reduction for 90% reliability (36 failed days) to an optimized cost of \$21,013.

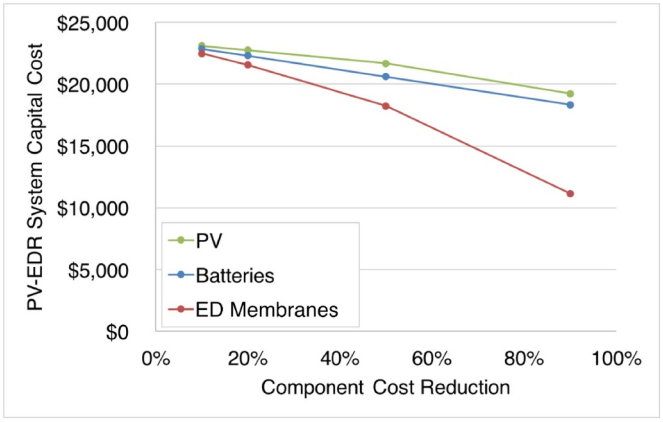

Fig. 10. Sensitivity of optimized PV-EDR system capital cost to individual component cost reductions of batteries, PV, and EDR membranes by 10%, 20%, 50% and 90%. For each data point, the cost of all other components is held constant at the previously defined cost values.

The optimization was also run for various reductions in component capital cost for the batteries, PV panels, and ED membranes. The impact of these component cost reductions on total system capital cost is shown in Fig. 10. For each curve in the figure, only the variable of interest was changed, with the others held constant. It is evident that the total system capital cost is most sensitive to the cost of the membranes, relative to the cost of batteries or PV panels.

4.3. Advantages of operation flexibility and membrane cost reductions for PV-EDR systems

The optimized PV-EDR system (Design A) had a predicted average operating time of 17.7 h per day. Desalination rate is proportional to the number of EDR membrane cell pairs that make up the EDR unit. To produce the necessary 10,000 L of product water per day, the optimized PV-EDR system was required to operate for this duration. Fig. 11 illustrates the frequency of number of required operation hours. The optimization converged on a design with a long operation schedule because it allowed for a smaller EDR unit, which was favorable due to the high capital cost of ED membranes.

It is not unreasonable to assume that in the future ED membrane costs will drop significantly compared to the current cost of the membranes used in the GE electrodialysis stack. In fact, according to supplier quotations from Hangzhou Iontech Environmental Technology in China, current prices for similarly sized ion-exchange membranes used in ED stacks are $40 per cell pair [47]. Since the membranes are approximately 0.64 m^2, this translates to a cost of $31.25/$m^2$ (two membranes per cell pair), more than 80% less than the cost of membranes from GE ($160/$m^2$). Electrodialysis membranes are a small market right now; their costs are likely to drop if demand increases and they are produced at greater economies of scale.

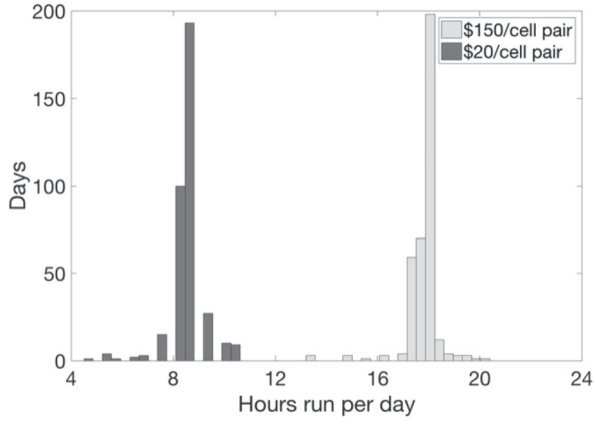

Fig. 11. Histogram of daily operating hours of PV-EDR systems optimized with $20 (average of 8.6 h per day) and $150 cell pair costs (17.7 h per day).

Table 8
Optimized PV-EDR design variables with $20 cell pairs and a total optimized system cost of $11,717. Due to the lower cell pair cost, ED stack size could be larger, decreasing the daily average operating time and thus could take advantage of the cost reductions associated with a flexible operating schedule.

Design variable	Symbol	Cost	Quantity
PV area	A_{PV}	$98/$m^2$	31 m^2
Battery capacity	E_{batt}	$150/kWh	5 kWh
Water storage volume	V_{tank}	$110/$m^3$	10 m^3
# ED cell pairs	N_{CP}	$20/cell pair	133 cell pairs
Stack voltage	v_{EDR}	N/A	95 V
Batch size	V_{batch}	N/A	0.68 m^3
Desalination rate	r_{desal}	N/A	1224 LPH
Daily operating time	t_{op}	N/A	8.6 h
Peak power	P_{pk}	N/A	2360 W
Total cost		$11,717	

To investigate the effect of significant, but reasonable, reductions in membrane cost, we performed the PV-EDR optimization using a membrane cell pair cost of $20. Lower cost cell pairs allow the ED subsystem to become less of the dominant cost driver in the system and balance with the PV subsystem. The optimized PV-EDR design with $20 per cell pairs costs $11,717 (Table 8). The size of the ED subsystem was larger than that in Table 4, enabling a higher flow rate in the stack and a reduced daily average operating time of 8.6 h.

This result is consistent with the findings of Watson et al. [31], which indicate that if the daily average operating time is closer to the number of sun hours available, the system can be driven more from the PV cells using less PV area, and will require less battery storage. All of these factors compound to reduce the system cost. A comparison of the hours operated per day for the EDR system optimized for $150 cell pairs and the system optimized for $20 cell pairs is shown in Fig. 11. The $20 per cell pair design has a shorter average operating time and a slightly wider spread of daily operating times, reflecting the increased operating flexibility allowed by operating exclusively during daylight hours compared to the optimized design with $150 cell pairs which has to operate at night. This case study of a PV-EDR system designed with $20 cell pairs supports the value of operation flexibility and load sizing for daytime operation, which are two methods of shaping the electrical load to better match the time-variant solar power profile [31].

5. Conclusions

In this study, the lowest capital cost village-scale, photovoltaic-powered electrodialysis desalination system for rural India was identified based on current component prices and performance. This was achieved through investigation of the parametric relationships that govern the characteristics of the electrodialysis process and the photovoltaic power system, and creation of a model to predict a PV-EDR system's performance. The model developed is generalized to take inputs of local conditions such as local feed water salinity, desired product water salinity, water demand profile, irradiance data and temperature data.

Through optimization, the cost-optimal system was predicted to be $23,420, a 42% reduction from the $40,138 cost of a PV-EDR system designed using convention methods of sequentially specifying the load

and then the power system. The optimized design consists of: an electrodialysis system using a GE ED stack with 62 cell pairs; an applied potential of 45 V; batch sizes of 0.42 m^3; a water storage tank of 10 m^3; a photovoltaic power system with 57.5 m^2 of PV panels; and 15.5 kWh of batteries. This design runs for an average of 17.7 h per day to provide the daily water requirement of 10 m^3. The production rate of water is low because there are relatively few cell pairs in the ED stack, a result of the cell pair cost being the dominant capital cost driver relative to other components. Therefore, by minimizing the number of cell pairs, the cost of the system could be reduced. It should be noted that the price of the optimized system is composed only of the major components that drive capital cost; future extensions of the work presented herein may need to consider smaller component costs (such as piping and the inverter for the electrical system), as well as operation costs.

Other optimal designs were generated and examined to investigate the parametric sensitivities of system capital cost to output reliability, feed and product water salinities, and individual component costs. It was found that relaxing the required output reliability from 100% to 98% reduced the capital cost of the system by approximately 5.7%. This strategy has diminishing returns; reducing the reliability by 10% only lowers the capital cost of the system by approximately 10.3%. This result indicates that a handful of days during the least sunny time of the year disproportionately drive up the system capital cost.

The high sensitivity of the optimal PV-EDR system design to the cost of membrane cell pairs prompted an investigation into how the PV-EDR system would change with $20 cell pairs instead of $150. It was found that the ED stack with $20 cell pairs was much larger compared to the optimal design with $150 cell pairs. This enabled the system to produce desalinated water faster and operate on average for fewer hours per day, closer to the timing of a normal work day. These results elucidated the value of operating the PV-EDR system during sunlight hours, in order to maximize the energy directly transferred from the PV panels to the system and minimize the required battery storage. Furthermore, this work shows that a flexible operation schedule is a cost-saving design strategy, enabling the system to produce more water on sunny days that can be used on cloudy days. This strategy effectively enables energy to be stored as excess water in tanks, which are a comparatively less expensive storage medium than batteries.

Nomenclature

α_p	temperature coefficient
A	active ED membrane area
A_{PV}	area of the photovoltaic panel array
C^0_{conc}	concentration of concentrate stream at the inlet of the ED stack
C_{conc}	concentration of the concentrate stream at the outlet of the ED stack
C^{wa}_{conc}	concentration on the surface of the anion exchange membrane at the boundary of the concentrate stream
C^{wc}_{conc}	concentration on the surface of the cation exchange membrane at the boundary of the concentrate stream
C^0_{dil}	concentration of the diluate stream at the inlet of the ED stack
C_{dil}	concentration of diluate stream at the outlet of the ED stack
C^{wa}_{dil}	concentration on the surface of the anion exchange membrane at the boundary of the diluate stream
C^{wc}_{dil}	concentration on the surface of the cation exchange membrane at the boundary of the diluate stream
C^{bulk}_{dil}	concentration of the bulk diluate solution
C_{batt}	specific battery cost
C_{CP}	ED membrane cell pair cost
C_{elec}	ED electrode cost
C_{pump}	pump cost
C_{sys}	total system capital cost
C_{tank}	specific water storage cost
D_a	average diffusion coefficient of NaCl in the anion exchange membrane
D_c	average diffusion coefficient of NaCl in the cation exchange membrane
η_{conv}	power converter efficiency
η_{PV}	photovoltaic panel efficiency
$\eta_{PV,nom}$	nominal photovoltaic panel efficiency
E_{batt}	battery energy capacity
E_{stored}	energy stored in the batteries
F	Faraday constant
GHI	global horizontal irradiance
I	current through the ED stack
i_{lim}	limiting current density
k	boundary-layer mass transfer coefficient or Ross coefficient
l_a	thickness of the anion exchange membrane
l_c	thickness of the cation exchange membrane
M_{pump}	pump model
N_{CP}	number of ED cell pairs
N_{failed}	number days the system fails to provide 10 m^3 of water
N_k	number of ED cell pairs
ϕ	current efficiency through the ED stack
p	pressure
P_{EDR}	power required for EDR over the course of a batch
P_{load}	load power draw
P_{pk}	peak load power
P_{pump}	pump power draw
P_{PV}	photovoltaic panel array power output
PSM	pump selection metric
Q	volumetric flow rate
Q_{conc}	volumetric flow rate of the concentrate stream
Q_{dil}	volumetric flow rate of the diluate stream
r_{req}	water production reliability
t	time
Δt	time interval
T	temperature
T_{amb}	ambient temperature
T_{mem}	transport number of the ion in the membrane
t_{op}	daily operating time
T_{std}	standard testing temperature (25° C)
TDS_{in}	input salinity
TDS_{out}	output salinity
t^+	transport number of the ion in the bulk solution
V_{batch}	EDR batch volume
v_{EDR}	ED stack voltage
V_k	volume of ED streams between ED cell pairs
V_{tank}	water storage tank volume
z	sign (+/−) and charge of the ion

Acknowledgments

This work was sponsored by Tata Projects Limited, the United States Agency for International Development (contract number AID-OAA-C-14-00185), the United States Bureau of Reclamation (agreement number R16AC00122), the MIT Energy Initiative, and the Tata Center for Technology and Design at MIT.

Appendix A

The following tables are the database of pumps that were considered in the optimization presented in this study, in order of increasing cost. The coefficients a, b and c relate the pump's output pressure p to the output flow rate Q by: $p = a + bQ + cQ^2$

Table 9

Manufacturer	Model	Volts (V)	Power (W)	Min Q (m^3/h)	Max Q (m^3/h)	Cost ($USD)	a	b	c
Kirloskar	Chhotu	12	370	0.36	1.98	27	30.44	−12.35	0
Kirloskar	JALRAAJ	12	370	0.36	2.12	39	34.64	−12.76	−0.35
Kirloskar	WONDER III	12	370	0.33	1.93	44	32.64	−14.37	0.29
Lubi	MDH-27ASF	12	820	0.9	2.28	45	35.64	−2.74	−3.93
Lubi	MDH-27N	12	370	0.85	2.7	46	38.16	−11.63	−0.38
Kirloskar	PEARL	12	370	0.4	2.25	47	27.76	−9.36	−0.14
Kirloskar	WAVE	12	370	0.33	1.93	50	32.64	−14.37	0.29
Kirloskar	STAR	12	370	0.45	2.7	52	32.52	−10.09	0.10
Kirloskar	V-FLOW	12	370	0.73	2.439	53	37.45	−1.95	−3.82
Kirloskar	JALRAAJ-1	12	750	0.25	3.28	54	44.77	−11.01	−0.25
Kirloskar	Crystal	12	750	0.65	3.2	57	37.84	−16.45	2.03
Lubi	MDH-12	12	370	2.7	6.6	57	9.14	5.66	−0.88
Kirloskar	Splash	12	750	0.5	3	57	30.67	−4.76	−1.15
Kirloskar	MINI-28S	12	370	0.72	3.15	62	34.23	−8.57	−0.13
Kirloskar	MINI 40S	12	750	0.2	3	66	43.29	−16.85	1.92
Kirloskar	POPULAR	12	750	0.2	3	66	42.07	−10.31	−0.13
Kirloskar	KSW-05	12	370	1.5	3.3	79	35.56	0.93	−3.09
Kirloskar	DC-4 M	12	550	2.16	5.76	84	25.26	1.08	−0.56
Lubi	MDH-14H	12	750	1.5	9.54	90	32.26	0.15	−0.22
Lubi	MDH-14S	12	750	2.1	6	90	35.20	−0.86	−0.32
Kirloskar	MINI 50S	12	750	0.78	3.73	91	66.90	−19.05	0.73
Kirloskar	V-FLOW 1	12	750	0.14	2.56	99	45.38	1.86	−6.74
Kirloskar	KDS-128	12	750	1.44	6.84	102	27.22	1.20	−0.46
Kirloskar	LIFTER-100	12	750	0.63	2.7	105	37.17	−0.71	−1.82
Kirloskar	LIFTER-150	12	1100	1.08	2.5	105	41.24	−3.90	−0.88
Kirloskar	LIFTER-50	12	370	0.5	2.3	105	21.35	3.02	−3.46
Kirloskar	LIFTER-60	12	370	0.6	2.6	105	24.25	14.34	−7.92
Kirloskar	MEGA 54S	12	1100	0.36	3.96	109	69.13	−16.20	0.32
Kirloskar	GMC-128	12	750	1.44	6.84	110	27.22	1.20	−0.46
Kirloskar	GMC-134	12	750	1.44	6	110	32.06	0.80	−0.58
Kirloskar	KDS-134	12	750	1.44	6	110	32.06	0.80	−0.58
Kirloskar	KJ-05V-H	12	370	0.36	1.92	118	38.47	−25.42	5.24
CNP	MS60-0.37	12	370	0	4.5	125	18.45	−1.18	−0.29
Kirloskar	GMC-1.540	12	1100	2.304	7.2	129	41.14	−0.75	−0.26
CNP	MS100-0.55	12	550	0	8.4	134	19.67	−0.89	−0.08
CNP	MS60-0.55	12	550	0	4.5	136	23.65	−1.41	−0.26
Lubi	MXF 101	12	750	1.2	7.2	138	26.25	−1.04	0
Kirloskar	KJ-10V-H	12	750	0.12	1.8	140	41.34	−19.72	0.98
Kirloskar	CMS140	12	750	0.5	2.57	143	25.54	32.39	−14.96
Kirloskar	CBR140	12	750	0.4 3	3.35	145	47.03	−11.55	−0.21
CNP	MS60-0.75	12	750	0	4.5	168	29.36	−1.52	−0.25
CNP	CHL2-30	12	550	0.5	3.5	169	29.49	−2.99	−0.41

Table 10

Manufacturer	Model	Volts (V)	Power (W)	Min Q (m^3/h)	Max Q (m^3/h)	Cost ($USD)	a	b	c
CNP	CHL2-50	12	550	0.5	3.5	173	47.75	−2.51	−1.37
Kirloskar	KJ-15V-H	12	1100	0.72	3.6	173	42.39	−8.78	−0.14
CNP	CHLF(T)2-30	12	550	0.5	3.5	175	29.10	−2.11	−0.62
CNP	CHLF(T)2-40	12	550	0.5	3.5	184	37.09	−1.66	−1.16
CNP	MS100-1.1	12	1100	0	9.6	196	29.32	−0.88	−0.09
CNP	CHLF(T)4-20	12	550	2	7	201	19.60	−0.15	−0.24
Grundfos	CM1-2	12	300	0.85	3	206	26.40	−1.54	−1.33
CNP	CHLF(T)4-30	12	550	2	7	211	27.74	0.34	−0.41
Grundfos	CM1-4	12	550	0.85	3	219	52.82	−3.37	−2.61
Grundfos	CM3-2	12	410	0.95	5.15	219	25.31	0.52	−0.58
CNP	CHLF(T)4-40	12	750	2	7	221	38.22	−0.02	−0.49
Grundfos	CM1-3	12	450	0.85	3	221	39.68	−2.58	−1.95
Grundfos	CM5-2	12	750	1.5	7.5	228	25.71	0.49	−0.22
Grundfos	CM3-3	12	630	0.95	5.15	239	38.10	0.99	−0.91
CNP	CHLF(T)2-50	12	550	0.5	3.5	239	47.83	−2.60	−1.35
CNP	CHLF(T)2-60	12	750	0.5	3.5	245	56.88	−5.13	−1.11
Grundfos	CM1-5	12	670	0.85	3	252	66.12	−4.51	−3.18

(continued on next page)

Table 10 (*continued*)

Manufacturer	Model	Volts (V)	Power (W)	Min Q (m^3/h)	Max Q (m^3/h)	Cost ($USD)	*a*	*b*	*c*
Grundfos	CM5-3	12	1100	1.5	7.5	254	38.43	0.91	−0.34
CNP	CHLF(T)4-50	12	1100	2	7	258	48.26	−1.10	−0.42
Grundfos	CM3-4	12	840	0.95	5.15	263	51.09	1.25	−1.20
Grundfos	CR1-2	12	160	0.23	2.91	269	17.73	2.02	−1.54
Grundfos	CR1s-2	12	100	0.11	1.3	269	17.29	0.74	−4.62
Grundfos	CR1-3	12	240	0.23	2.91	279	26.23	2.57	−2.29
Grundfos	CM1-6	12	780	0.85	3	285	79.26	−5.31	−3.87
Grundfos	CR1s-3	12	150	0.11	1.3	288	26.82	−2.91	−4.45
Grundfos	CM3-5	12	1040	0.95	5.15	289	64.00	1.55	−1.49
Grundfos	CR1s-4	12	200	0.11	1.3	295	35.27	−2.21	−7.39
Grundfos	CR1-4	12	320	0.23	2.91	300	35.13	3.07	−3.02
Grundfos	CR1-5	12	400	0.23	2.91	320	44.21	2.10	−3.29
Grundfos	CR3-2	12	250	0.34	5.41	320	18.25	0.65	−0.58
Grundfos	CR3-3	12	375	0.34	5.41	323	27.12	0.96	−0.82
Grundfos	CR1s-5	12	250	0.11	1.3	328	43.79	−3.88	−8.52
Grundfos	CM10-1	12	1100	3.5	18	330	24.62	−1.18	0.10
Grundfos	CR1s-6	12	300	0.11	1.3	336	52.85	−4.96	−10.29
Grundfos	CR3-4	12	500	0.34	5.41	339	36.29	1.00	−1.01
CNP	50-32-160-3	12	3000	0	25.92	341	28.76	−0.40	0
Grundfos	CR1-6	12	480	0.23	2.91	346	55.95	0.62	−3.67
Grundfos	CR5-2	12	460	0.68	10.22	348	20.36	−0.98	−0.02
CNP	65-50-160-0.55	12	550	0	21.6	349	7.56	0.05	−0.01
CNP	65-50-160-0.75	12	750	0	22.32	349	9.20	0.02	0
CNP	65-50-160-1.1	12	1100	0	25.2	349	10.79	0.06	−0.01
Grundfos	CR1s-7	12	350	0.11	1.3	355	57.53	0.92	−15.19
Grundfos	CR5-3	12	690	0.68	10.22	362	26.80	0.56	−0.23
Grundfos	CR3-5	12	625	0.34	5.41	370	44.37	1.21	−1.21
CNP	50-32-200-0.55	12	550	0	14.4	371	9.16	0.03	−0.01
CNP	50-32-200-0.75	12	750	0	15.84	371	11.44	0.07	−0.01
CNP	50-32-200-1.1	12	1100	0	17.28	371	13.98	0.15	−0.02
CNP	50-32-200-1.5	12	1500	0	18	371	18.03	0.10	−0.01

Table 11

Manufacturer	Model	Volts (V)	Power (W)	Min Q (m^3/h)	Max Q (m^3/h)	Cost ($USD)	*a*	*b*	*c*
Grundfos	CR1-7	12	560	0.23	2.91	372	55.08	8.72	−5.99
CNP	80-65-160-0.75	12	750	0	39.24	381	6.79	0	0
CNP	80-65-160-1.1	12	1100	0	41.76	381	9.05	0.03	−0.01
CNP	80-65-160-1.5	12	1500	0	44.64	381	11.31	0	0
CNP	65-40-200-1.1	12	1100	0	22.32	384	12.43	0.06	−0.01
CNP	65-40-200-1.5	12	1500	0	25.2	384	15.23	0.03	0
CNP	65-40-200-2.2	12	2200	0	26.64	384	17.20	0.03	0
CNP	ZS50-32-160-1.1	12	1100	3	12.5	387	19.40	−0.23	0
Grundfos	CR5-4	12	920	0.68	10.22	387	35.92	1.01	−0.34
Grundfos	CR1-8	12	640	0.23	2.91	390	114.79	−26.84	−0.08
CNP	80-50-200-1.5	12	1500	0	40.32	405	11.38	0.01	0
CNP	80-50-200-2.2	12	2200	0	46.08	405	15.11	0.02	0
CNP	80-50-200-3	12	3000	0	50.4	405	17.75	0.05	0
Grundfos	CR3-6	12	750	0.34	5.41	409	47.58	4.75	−1.82
CNP	ZS50-32-160-1.5	12	1500	3	18	419	22.43	−0.12	0
Grundfos	CR3-7	12	875	0.34	5.41	431	57.40	5.05	−2.06
Grundfos	CR5-5	12	1150	0.68	10.22	433	51.46	−1.93	−0.06
CNP	ZS50-32-160-2.2	12	2200	3	18	436	28.61	−0.18	−0.01
Grundfos	CR3-8	12	1000	0.34	5.41	447	57.69	8.90	−2.68
Grundfos	CR3-9	12	1125	0.34	5.41	460	115.88	−10.51	−0.98
CNP	65-40-250-1.5	12	1500	0	22.32	503	15.60	0.10	−0.01
CNP	65-40-250-2.2	12	2200	0	24.48	503	20.36	0.02	0
CNP	65-40-250-3	12	3000	0	25.2	503	25.00	0.05	−0.01
CNP	80-50-250-3	12	3000	0	43.2	530	19.13	0.04	−0.01
CNP	ZS50-32-200-3	12	3000	3	20	537	35.57	−0.22	0
Grundfos	CME1-2	12	300	0.85	3	567	26.74	−2.06	-1.22
CNP	SZ25-25-125	12	750	2.25	3.75	570	23.88	−0.93	−0.09
CNP	65-40-315-3	12	3000	0	21.6	582	26.71	0.05	0
Grundfos	CME1-3	12	410	0.85	3	582	39.58	−2.74	−1.89
Grundfos	CME3-2	12	410	0.95	5.17	582	25.30	0.41	−0.57
Grundfos	CME5-2	12	750	1.5	7.5	596	25.72	0.40	−0.20
Grundfos	CME1-4	12	520	0.85	3	600	52.58	−3.41	−2.60
Grundfos	CME3-3	12	650	0.95	5.17	615	38.25	0.78	−0.88
Grundfos	CME5-3	12	1100	1.5	7.5	622	38.46	0.96	−0.34

(*continued on next page*)

Table 11 (*continued*)

Manufacturer	Model	Volts (V)	Power (W)	Min Q (m^3/h)	Max Q (m^3/h)	Cost ($USD)	*a*	*b*	*c*
Grundfos	CME1-5	12	670	0.85	3	626	68.15	−6.29	−2.84
Grundfos	CME3-4	12	840	0.95	5.17	630	44.88	4.62	−1.63
Grundfos	CME1-6	12	800	0.85	3	663	79.07	−5.74	−3.71
Grundfos	CME1-7	12	910	0.85	3	674	111.63	−20.01	−2.06
Grundfos	CME3-5	12	1020	0.95	5.17	692	39.56	13.15	−2.83
Grundfos	CME10-1	12	1100	3.63	18	696	20.11	0.86	−0.13
Grundfos	BM 3A-9	12	550	0.8	4.35	2266	52.05	3.97	−2.85
Grundfos	BM 5A-5	12	625	3	7.8	2279	41.87	0.21	−0.38

References

[1] General Electric Water & Process Technologies, GE Aquamite EDR Systems Fact Sheet, Retrieved from the GE Water & Process Technologies Document Library website, (1998) https://www.gewater.com/kcpguest/document-library.do (Accessed May 19, 2017).

[2] N.C. Wright, A.G. Winter V. , Justification for community-scale photovoltaic powered electrodialysis desalination systems for inland rural villages in India, Desalination 352 (2014) 82–91.

[3] Datanet India Pvt. Ltd. Indiastat.com: Revealing India-Statistically: Statewise Distribution of Inhabited Villages According to Population of India. (Accessed November 10, 2013, as cited in Wright, 2014).

[4] P.H. Gleick, Basic water requirements for human activities: meeting basic needs, Water Int. 21 (2) (June 1996) 83–92.

[5] Bureau of Indian Standards, Drinking Water - Specification (Second Revision IS 10500), (2012) ISO 10500.

[6] Central Ground Water Board, Ground water quality in shallow aquifers of India, Technical report, Government of India, 2010.

[7] National Renewable Energy Laboratory, India Solar Resource, Direct Normal Irradiance, 2013 http://Www.Nrel.Gov/International/Images/India_Dni_Annual.Jpg (Accessed May 9, 2014, as Cited in Wright, 2014).

[8] Open Government Data Platform India, Data.Gov.In: Progress Report of Village Electrification as on May 2015, https://Data.Gov.In/Visualize/Inst=E66ecc8f79fbde7c078b6c5f497efb80 (Accessed February 28, 2017).

[9] C. Chandramouli, Census of India 2011 - household amenities and assets: source of lighting, Technical Report, Government of India, (2012).

[10] National Renewable Energy Laboratory, India SolarResource - Global Horizontal Irradiance, (2013) http://Www.Nrel.Gov/International/Images/India_Ghi_Annual.Jpg , Accessed date: 14 March 2017.

[11] C.B. Nataraja, Personal Conversation with Nataraja C. B. Tata Projects Water Purification Plant Development Center, Secunderabad, India, August 2016.

[12] P. Mehta, Impending Water Crisis in India and Comparing Clean Water Standards among Developing and Developed Nations, Scholars Research Library, Archives of Applied Science Research, 2012 available from http://www.scholarsresearchlibrary.com/articles/impending-water-crisis-in-india-and-comparing-clean-water-standards-among-developing-and-developed-nations.pdf . (Accessed May 15, 2017).

[13] A. Keller, R. Sakthivadivel, D. Seckler, ResearchReport 39: Water Scarcity and the Role of Storage in Development, International Water Management Institute, (2000).

[14] P. Chinnasamy, G. Agoramoorthy, Groundwater storage and depletion trends in Tamil Nadu State, India, Water Resour. Manag. 29 (7) (May 2015) 2139–2152.

[15] J. Ortiz, E. Exposito, F. Gallud, V. Garcia-Garcia, V. Montiel, A. Aldaz, Photovoltaic electrodialysis system for brackish water desalination: modeling of global process, J. Membr. Sci. 274 (1-2) (Apr. 2006) 138–149.

[16] M.R. Adiga, S. Adhikary, P. Narayanan, W. Harkare, S. Gomkale, K. Govindan, Performance analysis of photovoltaic electrodialysis desalination plant at Tanote in Thar Desert, Desalination, Desalination 67 (1987) 59–66.

[17] O. Kuroda, S. Takahashi, K. Wakamatsu, S. Itoh, S. Kubota, K. Kikuchi, Y. Eguchi, Y. Ikenaga, N. Sohma, K. Nishinoiri, An electrodialysis sea water desalination system powered by photovoltaic cells, Desalination 65 (1987) 161–169.

[18] N. Soma, F. Kanenobu, S. Inoue, O. Kuroda, The practical operation of photovoltaic desalination systems, Int. J. Sol. Energy 13 (1992) 97–109.

[19] Bloomberg New Energy Finance, The Cost Landscape of Solar and Wind, Bloomberg database, January 2015.

[20] A. Bilton, Modular Design Architecture for Application to Community-Scale Photovoltaic-Powered Reverse Osmosis Systems, Massachusetts Institute of Technology, Cambridge, Massachusetts, 2006 Doctor of Philosophy thesis.

[21] A. Bilton, S. Dubowsky, Modular design of community-scale photovoltaic reverse osmosis systems under uncertainty, Proceedings of the ASME, 40th Design Automation Conference, 2014.

[22] A. Bilton, A Modular Design Architecture for Application to Community-Scale Photovoltaic-Powered Reverse Osmosis Systems, Cambridge, 2006.

[23] A.M. Bilton, L.C. Kelley, Design of power systems for reverse osmosis desalination in remote communities, Desalin. Water Treat. 55 (10) (2015) 2868–2883, https://doi.org/10.1080/19443994.2014.940641.

[24] E. Koutroulis, D. Kolokotsa, Design optimization of desalination systems power-supplied by PV and W/G energy sources, Desalination 258 (1) (2010) 171–181.

[25] N.C. Wright, S.R. Shah, S.E. Amrose, V.A.G. Winter, A Robust Model of Brackish Water Electrodialysis Desalination with Experimental Comparison at Different Size Scales, Desalination 443 (2018) 27–43.

[26] N.C. Wright, G.D. Van de Zande, A. Winter, Design of a Village-Scale PV Powered Electrodialysis Reversal System for Brackish Water Desalination in India, The International Desalination Association World Congress on Desalination and Water Reuse, San Diego, CA, USA, 2015.

[27] J.M. Ortiz, J.A. Sotoca, E. Exposito, F. Gallud, V. Garca-Garca, V. Montiel, A. Aldaz, Brackish water desalination by electrodialysis: batch recirculation operation modeling, J. Membr. Sci. 252 (1-2) (2005) 65–75.

[28] H. Strathmann, Electrodialysis, a mature technology with a multitude of new applications, Desalination 264 (3) (2010) 268–288.

[29] Y. Tanaka, Ion Exchange Membrane Electrodialysis: Fundamentals, Desalination, Separation, Nova Science Publishers, 2010.

[30] General Electric Water & Process Technologies, New High-Performance Spacer in Electrodialysis Reversal (EDR) Systems, (1998) Retrieved from the GE Water & Process Technologies Document Library website https://www.gewater.com/kcpguest/document-library.do . (Accessed October 3, 2016).

[31] S. Watson, D. Bian, N. Sahraei, A. Winter, T. Buonassisi, I.M. Peters, Advantages of Operation Flexibility and Load Sizing for PV-Powered System Design, Solar Energy 162 (2018) 132–139.

[32] S.M. Watson, Cost Optimization of a Solar-Powered Electrodialysis Desalination System, Massachusetts Institute of Technology, Cambridge, Massachusetts, 2017 Master's thesis.

[33] National Renewable Energy Laboratory (NREL), Latitude: 17.84, Longitude: 79.35, Country: India, Year: 2014, https://maps.nrel.gov/nsrdb-viewer/ (Accessed September 20, 2016).

[34] Suniva Optimus Series Monocrystalline Solar Modules, [Online] Available from https://Www.Wholesalesolar.Com/Cms/Suniva-Suniva-Opt330-72-4-100-Silver-Mono-Solar-Panel-Specs-1610309543.Pdf. (Accessed May 20, 2016).

[35] The Performance of Photovoltaic (PV) Systems: Modeling, Measurement and Assessment, No. 105, in: N. Pearsall (Ed.), Woodhead Publishing, 2017.

[36] A. Rose, A. Campanella, R. Amatya, R. Stoner, Solar Power Applications in the Developing World, The MIT Future of Solar Energy Study Working Paper, January 2015.

[37] Private Participation in Renewable Energy Database: Solar, World Bank, http://ppire.worldbank.org/snapshots/technology/solar#regional-breakdown, (2013) (Accessed December 5, 2016).

[38] General Electric Water & Process Technologies, Supplier Quotations for Ion Exchange Membranes, (2014) Westborough, MA.

[39] N.S. Shrikhande, Personal Conversation with Nilesh S. Shrikhande, Tata Power Solar, Bangalore, India, July 2016.

[40] C.B. Nataraja, Personal Conversation with Nataraja C. B. Tata Projects Water Purification Plant Development Center, Secunderabad, India, May 27, 2016.

[41] MATLAB, The MathWorks, Inc. Natick, Natick, Massachusetts, United States, 2016.

[42] J. Kennedy, R. Eberhart, Particle swarm optimization, Proceedings of the IEEE International Conference on Neural Networks, Perth, 1995.

[43] V.H. Lienhard, A. Bilton, M.A. Antar, G. Zaragoza, J. Blanco, Solar desalination, Annual Review of Heat Transfer, vol. 15, Begell House, Inc., New York, 2012.

[44] J.E. Miller, Review of Water Resources and Desalination Technologies, Sandia National Laboratories, Albuquerque, NM, 2003 (49 pp.) URL http://prod.sandia.gov/techlib/access-control.cgi/2003/030800.pdf (Accessed May 19, 2017).

[45] K.S. Spiegler, Y.M. El-Sayed, A Desalination Primer, Balaban Desalination Publications, Santa Maria Imbaro, Italy, 1994.

[46] How to Design Solar PV System, http://www.leonics.com/support/article2_12j/articles2_12j_en.php, (2013) , Accessed date: 15 March 2017.

[47] Hangzhou Iontech Environmental Technology Company Limited, Supplier Quotations for Ion Exchange Membranes, (2014) Hangzhou, China.